Carbohydrate Polymers 98 (2013) 711–720

Contents lists available at SciVerse ScienceDirect

Carbohydrate Polymers

journal homepage: www.elsevier.com/locate/carbpol

Starch-based microspheres for sustained-release of curcumin: Preparation and cytotoxic effect on tumor cells

Antonio G.B. Pereira [a,*], André R. Fajardo [a], Samara Nocchi [b], Celso V. Nakamura [b], Adley F. Rubira [a], Edvani C. Muniz [a]

[a] Grupo de Materiais Poliméricos e Compósitos (GMPC) – Chemistry Departament, Maringa State University, Av. Colombo 5790, 87020-900 Maringá, Paraná, Brazil

[b] Laboratório de Microbiologia Aplicada aos Produtos Naturais e Sintéticos and Laboratório de Inovação Tecnológica no Desenvolvimento de Fármacos e Cosméticos – Clinical Analysis Departament, Maringa State University, Av. Colombo 5790, 87020-900 Maringá, Paraná, Brazil

ARTICLE INFO

Article history:
Received 21 March 2013
Received in revised form 12 June 2013
Accepted 13 June 2013
Available online 24 June 2013

Keywords:
Microspheres
Starch
Curcumin
Oral drug delivery system
Antitumor activity

ABSTRACT

Curcumin (CUR) has been proved to be highly cytotoxic against different tumor cell lines. However, its poor solubility in aqueous medium and fast degradation in physiological pH are the common drawbacks preventing its efficient practical use. Herein, we report the development of original microspheres based on the biopolymer starch crosslinked with N,N-methylenebisacrylamide (MBA) to be applied as an efficient delivering system for CUR. The starch-based microspheres showed high loading efficiency even in loading solution with different CUR concentrations. In vitro release assays data showed that the CUR release is governed by anomalous transport ($n = 0.73$) and it is pH-dependent. Cytotoxicity assays showed that starch microspheres could improve the cytotoxicity of CUR toward Caco-2 and HCT-116 tumor cell lines up to 40 times than that found for pure CUR. This behavior was attributed to the slowly and sustained release of CUR from the microspheres.

© 2013 Elsevier Ltd. All rights reserved.

1. Introduction

Curcumin, *1,7-bis-(4-hydroxy-3-methoxy-phenyl)-hepta-1,6-diene-3,5-dione*, is a natural pigment derived from an active component of *curcuma longa* (Mandeville, Froehlich, & Tajmir-Riahi, 2009; Tang et al., 2010). It has been demonstrated by several studies that curcumin (CUR) has a wide range of biological and pharmacological activities, especially against cancer propagation and prevention (Cabrespine-Faugeras, Bayet-Robert, Bay, Chollet, & Barthomeuf, 2010; Radhakrishna Pillai, Srivastava, Hassanein, Chauhan, & Carrier, 2004). Although, CUR has great efficiency in the treatment of some human tumors its water insolubility and instability limits its application (Anand, Kunnumakkara, Newman, & Aggarwal, 2007). The hydrophobic nature disables, for instance, its vascular and oral administration (Sharma, Gescher, & Steward, 2005). One alternative to overcome such limitations is the application of an adequate releasing system (hydrogels, dendrimers, liposome, micro, and nanoparticles) for CUR delivering. The employment of such systems in controlled drug delivery has been widely explored for long time (Sun, Shoji, Lu, Liotta, & Snyder, 2006; Vemula, Cruikshank, Karp, & John, 2009). A variety of polymeric materials (synthetic and natural) have been used to synthesize/prepare efficient carriers (Jain, Gupta, & Jain, 2007; Saito et al., 2005). That was possible because polymeric materials include a huge variety of molecules, which can enable adhesion at the delivered site and allow the sustained drug release. Additionally, functional components can be combined with the polymeric carrier to target the drug or to control the releasing rate, for instance.

A promising natural polymer widely applied in several fields that shows interesting physical, chemical and biological features is starch. Starch is a complex polysaccharide composed by amylose and amylopectin, two macromolecules that have different characteristics. Amylose is a linear macromolecule consisting of α-D-glucopyranose units linked through (1 → 4) linkages and has a molecular weight of 10^5–10^6 g/mol. Amylopectin is a branched macromolecule formed by short chains linking linear chains via (1 → 6) linkages and has molecular weight of 10^6–10^7 g/mol (Namazi & Dadkhah, 2010) that possesses hydrophilic nature. It is important to emphasize that starch has natural abundance, low cost of production, renewability, biocompatibility and biodegradability, features that support its application in the development of drug delivery systems. In order to improve and/or create its end-use properties, starch can be chemically modified (Angellier, Molina-Boisseau, Dole, & Dufresne, 2006; Xu et al., 2010). One starch modification example is the introduction of chemical groups on the

* Corresponding author. Tel.: +55 44 30313676; fax: +55 44 30313676.
E-mail address: guilebasso@hotmail.com (A.G.B. Pereira).

0144-8617/$ – see front matter © 2013 Elsevier Ltd. All rights reserved.
http://dx.doi.org/10.1016/j.carbpol.2013.06.013

starch chains to allow its crosslinking with other polymer (Kim, Cho, & Park, 2001). The crosslinked network improves considerably the mechanical properties and the water resistance of starch-based materials. Furthermore, some reports show that crosslinked starch chains acquires resistance against enzymatic hydrolyzes enabling it to be used, for instance, as carrier in oral drug delivery systems (Chen et al., 2007; Reis et al., 2008). Taking into account these considerations, we present the development and characterization of original microspheres based on chemically modified starch crosslinked with *N,N′*-methylenebisacrylamide (MBA) to act as an efficient deliverer of CUR.

2. Materials and methods

2.1. Materials

Cassava starch was kindly supplied by INPAL S.A. (São Tomé, Brazil) M_w 5.4×10^3 kDa determined by GPC/SEC as described elsewhere (Pereira, Gouveia, de Carvalho, Rubira, & Muniz, 2009). Glycidyl methacrylate (GMA, 97% CAS: 106-91-2), curcumin from *curcuma longa* (Turmeric) (CUR, CAS: 458-37-7), sodium dodecyl sulfate (SDS, CAS: 151-21-3), and sodium persulfate (SPS, CAS: 7775-27-1), were purchased from Sigma–Aldrich (St. Louis, USA). Sunflower oil (CAS 8001-21-6) was purchased from Cocamar (Maringá, Brazil). *N,N*-methylenebisacrylamide (MBA, CAS: 110-26-9) was purchased from Biorad (Hercules, USA); and sodium hydroxide (NaOH, 95%, CAS: 1310-73-2), acetone (99.5%, CAS: 67-64-1), absolute ethanol (99.5%, CAS: 64-17-5), hexane (99%, CAS 110-54-3), dimethyl sulfoxide (DMSO, 99%, CAS 67-68-5), and tetrahydrofuran (THF, CAS 109-99-9) were purchased from Nuclear (São Paulo, Brazil). All materials and reagents were used as received.

2.2. Synthesis of chemically modified starch (starch-mod)

Starch was chemically modified adapting the methodology developed by Reis et al. (2008). Briefly, starch (4 g) was solubilized in distilled water/DMSO mixture (ratio 1:1) at 80 °C under vigorous stirring. After complete solubilization, the temperature was reduced to 60 °C and the pH was adjusted to 10.5 with NaOH solution (0.2 M). GMA (4 ml) was added to the reaction system, which was kept under mechanic stirring at 60 °C for 24 h. The chemically modified starch (starch-mod) was recovered by precipitation in ethanol. The precipitated material was separated by vacuum filtration. At last, the starch-mod was washed several times with ethanol and water portions to complete eliminate unreacted materials and then it was lyophilized (at −55 °C and 0.1 mBar for 12 h).

2.3. Starch-mod characterization

2.3.1. Fourier transform infrared spectroscopy (FTIR)

FTIR spectra of raw starch, GMA, and starch-mod was recorded using a Shimadzu 8300 FTIR spectrophotometer operating in the region from 4000 cm^{-1} to 500 cm^{-1} with resolution of 4 cm^{-1} and 64 scan acquisitions. The dried samples were mixed with KBr powder and pressed into pellets for spectrum acquisition.

2.3.2. Nuclear magnetic resonance (NMR)

^1H NMR spectra of raw starch, GMA, and starch-mod were recorded on Varian 300 MHz unity (Oxford, model 300). Approximately, 10% sample solutions in DMSO-d_6 (raw starch and starch-mod samples) and $CDCl_3$ (GMA sample) were prepared in 5 mm tubes with samples referred to tetramethysilane (the tetramethysilane signal was suppressed from the ^1H NMR spectra). Chemical shifts in ppm were obtained by first-order analysis of spin patterns (here it was considered that the proton is only coupled to other protons that are far away in chemical shift) for ^1H NMR experiments with the following conditions: number of data points 12 K; relaxation delay 30 s; angle pulse 90°; acquisition time 5 s; temperature 298 K; number of scans 32.

2.4. Microspheres preparation

Microspheres based on modified starch (starch-mod) crosslinked with MBA were prepared in water/oil emulsion system. 2 g of starch-mod were dissolved in distilled water (90 ml) at 80 °C to form the aqueous phase. The solution was cooled to room temperature and MBA (40 mg) and SPS (0.25 mg) were added. The oleaginous phase, composed by sunflower oil (90 ml), was deposited in a round bottom flask coupled to a mechanical stirrer apparatus. Sodium dodecyl sulfate (SDS – 3.5 g) was added as emulsifier and the system was stirred for 15 min (1000 rpm) before the temperature was increased to 90 °C. Both phases were deoxygenated through N_2 bubbling for 15 min. The aqueous phase was poured slowly to the oil phase, and then the stirring was increased to 2000 rpm and kept for 30 min to crosslink. Finally, the system was cooled to room temperature and the microspheres were recovered by filtering under vacuum. The recovered microspheres were washed several times successively with portions of hexane (2× 20 ml) to eliminate some oil residue, acetone (2× 20 ml), ethanol (2× 20 ml) and water (2× 20 ml) to eliminate the non-reacted chemicals (MBA, sodium persulfate, SDS, starch-mod). Then, microspheres were lyophilized before analyses.

2.5. Microspheres characterization

2.5.1. Scanning electron microscopy (SEM)

The morphology was investigated by SEM images (Shimadzu, model SS 550, Japan). The microspheres were sputter-coated with a thin layer of gold and image acquisition was taken by applying an electron accelerating voltage of 12 kV. The microspheres average diameter was calculated by the Size Meter© software with differentiation threshold set according to the image scale.

2.5.2. Fourier transform infrared spectroscopy (FTIR)

FTIR spectroscopy and analytical procedures were performed according to parameters described in the previous section.

2.5.3. Thermogravimetry (TGA)

TGA was performed on freeze-dried samples from 25 °C to 600 °C at a heating rate of 10 °C/min under 30 ml/min of flowing N_2 in a thermogravimetric analyzer (Netzch, model STA 409 PG/4/G Luxx, USA).

2.6. Curcumin loaded microspheres

CUR (1.25 mg) was solubilized in water/THF (ratio 1:1, 100 ml) to prepare the stock solution. After, 1.0 g of microspheres was deposited in that solution. The system microspheres/CUR stock solution was kept under magnetic stirring overnight at room temperature. So, the loaded microspheres were removed by high-speed centrifugation and oven-dried at 40 °C for 24 h. The stock solution was analyzed through UV spectroscopy technique to evaluate the loading efficiency. The supernatant was analyzed at 430 nm using a UV-Vis Femto (model 800Xi, Brazil) apparatus. Using a previously built analytical curve, the concentration of CUR remaining in the supernatant was calculated. The analytical curve was designed from standard CUR solutions varying from 0.17 to 7.68 mg/l using water/THF (ratio 1:1) as solvent. The linear correlation coefficient

(R^2) value was higher than 0.999. The encapsulation efficiency was calculated using the following equation:

$$\text{Encapsulation efficiency } (\%) = \frac{[CUR_0] - [CUR_s]}{[CUR_0]} \times 100 \quad (1)$$

where $[CUR_0]$ is referent to initial amount of curcumin and $[CUR_s]$ is the amount of curcumin remaining in the supernatant.

2.7. CUR release assays

The in vitro CUR release assays were performed in two different environments: simulated intestinal fluid [SIF, 6.8 g KH_2PO_4 and 77 ml aqueous NaOH (0.2 M) in water – final pH = 6.8, 1000 ml] and simulated gastric fluid [SGF, 2.0 g NaCl and 7.0 ml HCl (37 g/g%) in water – final pH = 1.2, 1000 ml], both without the presence of enzymes. The release assays were carried out in a dissolution apparatus in which for each fluid 200 mg of dry loaded microspheres were deposited in a sealed flask with 150 ml of SIF or SGF. The release study was carried out in triplicate ($n = 3$) for a given fluid. After the dipping of each sample in a desired fluid, the system was kept under constant stirring (75 rpm) at 37 °C over whole test. At a desired time interval, an aliquot (ca. 5 ml) was removed from each flask to quantify, through UV measurements, the amount of drug released as described previously. The aliquots were centrifuged before the UV analysis to avoid the interference of microspheres. After the UV measurements those aliquots and the precipitated were replaced into their respective flask. The analytical curves for CUR in SGF and in SIF were built in the concentration range of 0.03–3.0 mg/l. R^2 values were as high as 0.999 for both analytical curves.

2.8. Cytotoxic effect on tumor cell lines

Caco-2 and HCT-116 cell lines, originated from a human colonic adenocarcinoma and human corectal carcinoma, were cultured and maintained in Dulbecco's modified Eagle's medium (DMEM; Gibco®, Grand Island, NY, USA) supplemented with 10% heat-inactivated fetal bovine serum (FBS; Gibco®) and 50 μg/mL gentamycin, in incubator set at 37 °C, 5% CO_2 and 95% relative humidity. The cells were expanded when monolayer reached confluence after 3. After reaching 80% confluence, cells were digested by using 0.25% trypsin (Gibco®) contained 1 mM EDTA.

The cytotoxic effect of the CUR released from microspheres on the Caco-2 and HCT-116 cell lines were determined by sulforhodamine B test (SRB-test) (Skehan et al., 1990). The unloaded microspheres were utilized as control and pure CUR was tested as a comparative. In addition, two sets of microspheres with different amount of encapsulated CUR were tested. The first one (labeled as C1) was loaded in a CUR solution with concentration equal to 1 mg/ml and the second (labeled as C100) in a CUR solution with concentration equal to 100 mg/ml. The encapsulation efficiency was equal to 80.54% to C1 (0.81 mg of CUR encapsulated in 1 g of microspheres – 0.085 wt/wt%) and 82.38% to C100 (82.38 mg of CUR encapsulated in 1 g of microspheres – 8.24 wt/wt%), respectively. The experimental procedures for encapsulating CUR for evaluating the encapsulation efficiency were the same described above.

The cells were seeded in 96-well tissue plates (TPP – Techno Plastic Products, Trasadingen, Switzerland) at a density of 8×10^5 cell/ml in 100 μl of medium for 24 h in the CO_2 incubator. For each sample (control, pure CUR, C1, and C100) solutions with different concentrations (500, 100, 10, 1, and 0.1 μg/ml) were prepared and added to the culture media. After incubation for 48 h, the cell monolayers were washed with 100 μl phosphate buffered saline (PBS) sterile, fixed with trichloroacetic acid and stained for 30 min with SRB (7.16 mmol/l) (Sigma Chemical Co., St. Louis, MO, USA) in acetic acid solution. The dye was removed by four washes with acetic acid solution (175 mmol/l), and protein-bound dye was extracted with 10 mM unbuffered Tris base [tris(hydroxymethyl)aminomethane] for determination of optical density in a computer-interfaced, 96-well microtiter plate reader (Power Wave XS, BIO-TEK®, Winooski, VT, USA). The CC_{50} values were determined from a percentage of cells relative to untreated control and the half-life of the Caco-2 and HTC cells in the presence and absence of each tested sample was estimated as the time point at which the cell viability decreased to 50% in relation to the beginning of the test. All the tests were performed in triplicate ($n = 3$).

3. Results and discussion

3.1. Starch modification

Raw starch was chemically modified with GMA to introduce in its backbone methacrylate groups enabling further radical polymerization and the formation of a crosslinked network. The insertion of methacrylate groups from GMA on different polysaccharides backbones is a well-known methodology used to form crosslinked networks (Guilherme et al., 2012; Thompson et al., 2006). The chemical reaction of GMA with the polysaccharide has been described in the literature by two possible mechanism routes. The first is the transesterification reaction forming the methacrylated-polysaccharide and glycidol as byproduct. The transesterification predominates when the reaction is carried out in an aprotic solvent, as DMSO, and usually is classified as fast and reversible. The second route is the epoxy ring-opening mechanism, which forms two products according to the opening site of the epoxide ring. This route predominates when the reaction is carried out in a protic solvent, as water. The epoxy ring-opening reaction is known as slow and irreversible, fact that could increase its effectiveness (Guilherme et al., 2012; Thompson et al., 2006). Fig. 1 shows a reaction scheme for the chemical modification of raw starch with GMA.

Fig. 2a shows the FTIR spectra of raw starch, GMA, and starch-mod. The FTIR spectrum of raw starch shows the stretching vibration of hydroxyl groups at 3405 cm^{-1}, the C—H stretching at 2953 cm^{-1}, the scissoring of two —OH bond adsorbed water molecules at 1653 cm^{-1}, the asymmetric vibration of the C—O—C bond and C—O vibration at 1157 and 1017 cm^{-1} (Riyajan, Sasithornsonti, & Phinyocheep, 2012; Zhang et al., 2012). The FTIR spectrum of GMA shows the C—H stretching at 3003, 2962, and 2929 cm^{-1} assigned to CH_2 and CH_3 groups, the C=O and C=C stretching from the ester conjugated system at 1718 and 1650 cm^{-1}, the C—O—C stretching of the epoxide group at 909 cm^{-1}, and the =C—H stretching at 811 cm^{-1} (Guilherme et al., 2005; Meng, Yuan, Rong, & Zhang, 2010).

The starch-mod FTIR spectrum, differently from the raw starch spectrum, shows a shoulder at 1718 cm^{-1} assigned to C=O proceeding from GMA (Hedin, Östlund, & Nydén, 2010; Reis et al., 2008). In addition, it is possible to observe a slight increase in the intensity of the band at 1650 cm^{-1}, which is due to overlapping of the C=C stretching and scissoring of OH bond from absorbed water molecules proceeding from the raw starch. This indicates the successful chemical modification of the raw starch by GMA (Hedin et al., 2010; Reis et al., 2008). Furthermore, in the starch-mod spectrum there is an increase of intensity in the spectral region of 1450–1350 cm^{-1} due to C—H bend, which characterizes the insertion of CH_2 and CH_3 groups into starch backbone. At last, the spectral region of 1200–1000 cm^{-1} in the starch-mod spectra exhibits a slight increase of intensity due to C—O stretching frequency groups. All these evidences confirm the modification of raw starch by GMA (Hedin et al., 2010; Reis et al., 2008).

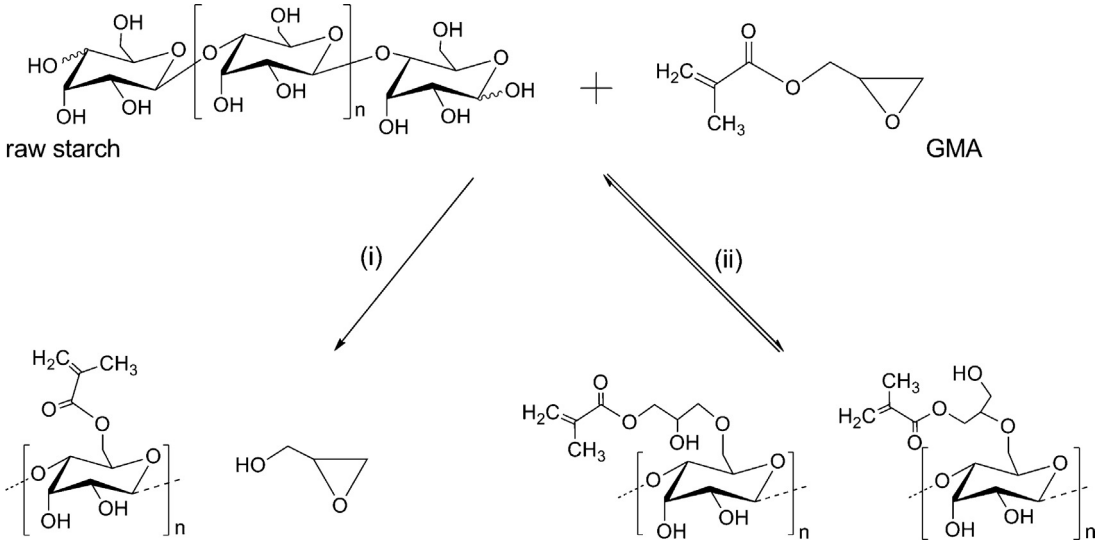

Fig. 1. Reaction scheme for the chemical modification of raw starch with GMA. (i) Epoxy ring-opening and (ii) transesterification routes.

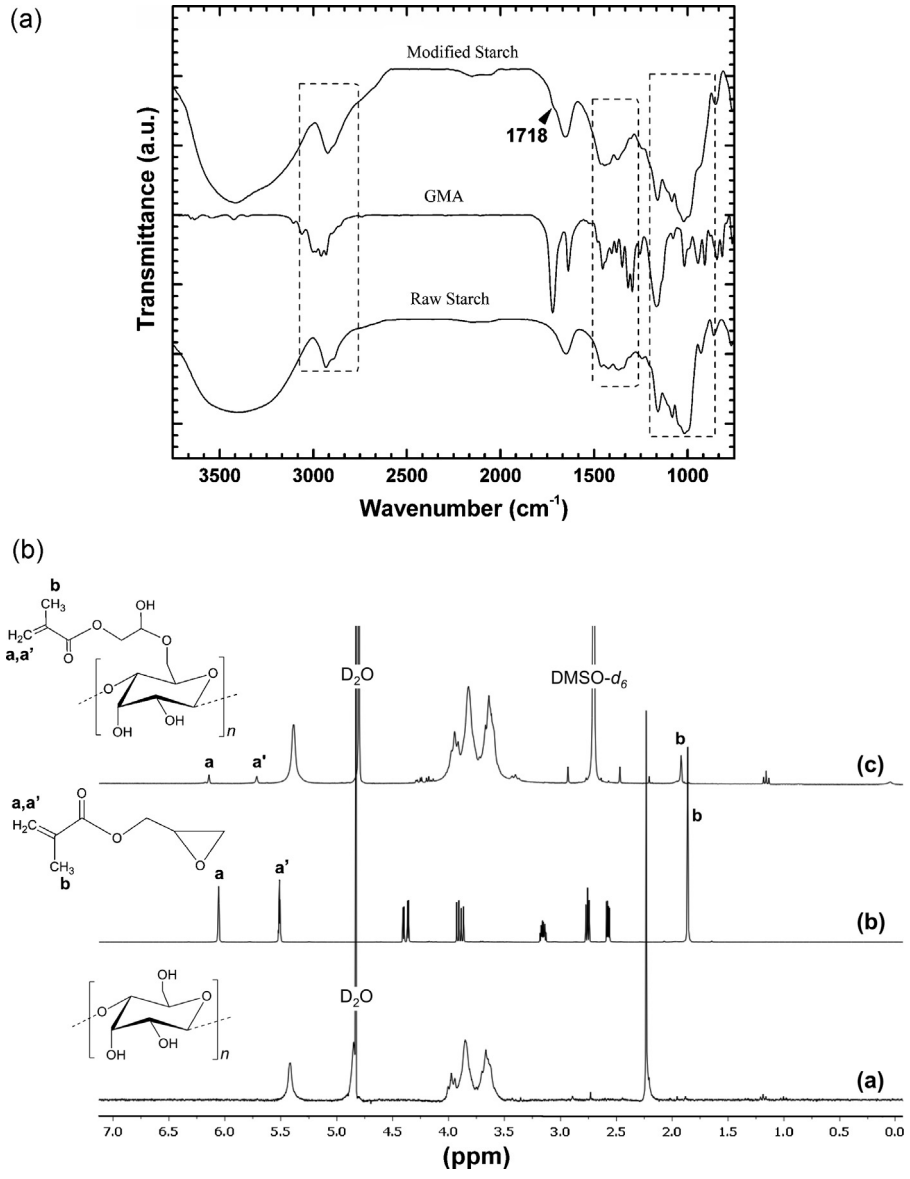

Fig. 2. (a) FTIR and (b) ^{1}H NMR spectra of raw starch, GMA and modified starch.

^{1}H NMR spectra of raw starch, GMA, and starch-mod are shown in Fig. 2b. The resonance signals at chemical shifts (δ) 6.16 and 5.71 ppm (denoted as a and a') in the starch-mod spectrum are evident, and can be attributed to hydrogen bounded to vinyl group coming from reaction with GMA. Moreover, an intense resonance signal at δ 1.96 ppm (denoted as b) can be observed in the starch-mod spectrum. This signal is attributed to hydrogen bounded to methyl groups from GMA. All these resonance signals that appeared in the starch-mod spectrum corroborate with the results found in other works that dealt with chemical modification of starch with GMA (Hedin et al., 2010; Reis et al., 2008). According to some studies, the insertion of methacrylate groups from GMA into starch backbone could happen by both transesterification and epoxy ring-opening mechanism routes according to the solvent used. In this work, the chemical modification of raw starch by GMA was performed in a mixture of solvents (DMSO/water), which might suggest that both mechanism routes could happen (Reis et al., 2008, 2009; Sahu, Bora, Kasoju, & Goswami, 2008). However, as mentioned, the epoxy ring opening, characterized as a slow and irreversible reaction, is more effective than transesterification reaction and, therefore was the preferential pathway for such reaction (Reis et al., 2008, 2009; Sahu et al., 2008). The success of this mechanism route is confirmed by the appearing of just two-resonance signals in the starch-mod spectrum that are assigned to hydrogen bounded to vinyl group from GMA inserted into starch backbone.

The degree of substitution (DS) of raw starch by reaction with GMA was determined from the starch-mod ^{1}H NMR spectrum. For this, Eq. (2) was utilized (Hedin et al., 2010):

$$\mathrm{DS} = \frac{(I_{\delta 6.16} + I_{\delta 5.71})/2}{I_{\delta 5.39}} \quad (2)$$

This equation relates the total areas of the two-resonance signal assigned to the vinyl hydrogens (δ 6.16 and 5.71 ppm) observed in the spectrum of the starch-mod to the resonance signal at δ 5.39 ppm observed in the spectrum of the raw starch, which is assigned to the hydrogen bond to the anomeric carbon in the glucose unit (Hedin et al., 2010). The respective areas of the resonance signals were measured after a careful baseline treatment and the respective values are $I_{\delta 6.16} \approx 1.07$; $I_{\delta 5.71} \approx 1.0$; and $I_{\delta 5.39} \approx 12$. Inserting these values in the equation 2 the DS calculated for starch-mod is 8,7%. This is a lower DS as compared to the results presented by Hedin et al., which studied this same modification in DMSO medium (Hedin et al., 2010). Some works associate higher DS values for modification of the amylose moiety of starch, while the modification of amylopectin does not reproduce the same good results (Huang, Schols, Klaver, Jin, & Voragen, 2007).

3.2. Microspheres preparation

Starch modified by reacting with glycidyl methacrylate is supposed to form a network by itself without the need of further crosslinker. However, the use of MBA as an additional crosslinker was necessary due to the low DS obtained in the modification reaction of starch. MBA has been used in several devices aiming biomedical application and has been proven to be safe as crosslinker (Costa et al., 2011; Mandal, Kapoor, & Kundu, 2009). Therefore, the use of MBA in the preparation of starch-mod microspheres does not compromise its potential as a device for drug delivery system. Although many studies (Kim et al., 2001; Rodrigues et al., 2012; Spagnol, Rodrigues, Pereira, et al., 2009; Spagnol, Rodrigues, Neto, et al., 2009) report the effect of crosslinker on swelling properties of three-dimensional networks based on different polymeric matrix, such aspect was not focused in this manuscript.

From SEM images (Fig. 3), the average size of microspheres was determined to be between 400 and 500 μm. The microspheres show a rough surface and some bulges outward, which can be attributed to the dragging of material from the interior during the purification and the drying process.

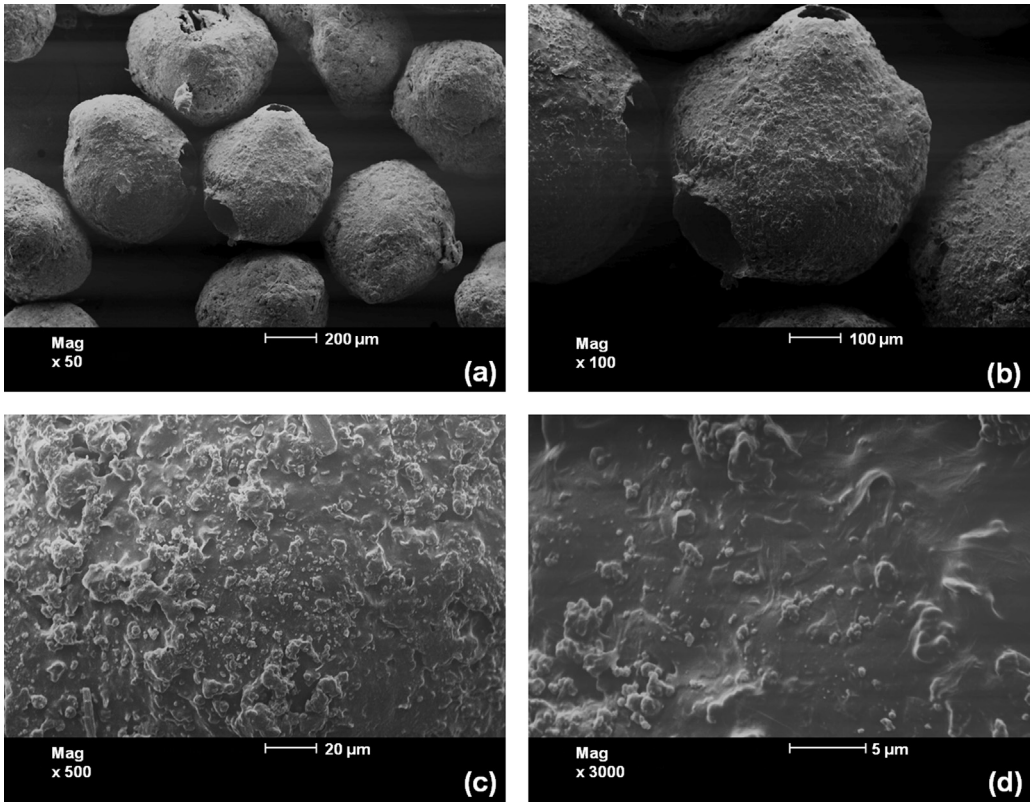

Fig. 3. SEM images of microspheres (a and b) and microspheres surface (c and d).

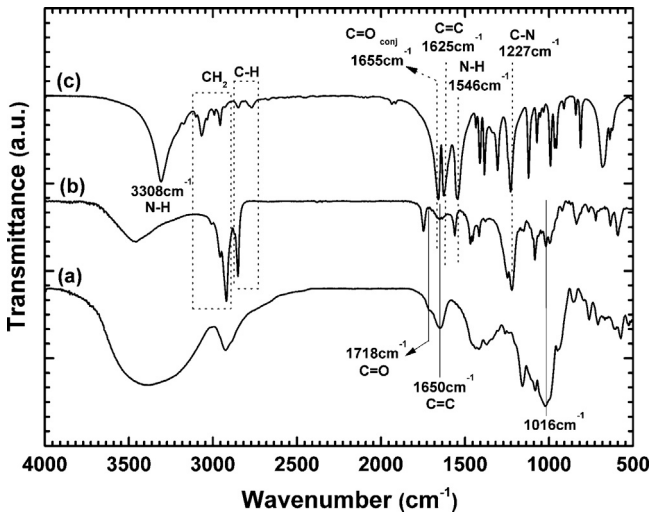

Fig. 4. FTIR spectra of (a) starch-mod, (b) microspheres and (c) MBA.

Fig. 4 shows the FTIR spectra for starch-mod, MBA and the microspheres. The starch-mod FTIR spectrum shows a band at 1718 cm^{-1} assigned to C=O vibrational stretching. The vibrational stretching attributed to the C=C bond should appear at ca. 1650 cm^{-1}, however a broad signal appears in that region attributed to water adsorbed in the amorphous regions of starch (Kizil, Irudayaraj, & Seetharaman, 2002). MBA FTIR spectrum shows a broad intense band at 3308 cm^{-1} assigned to N–H vibrational stretching; bands at 1655 and 1650 cm^{-1} assigned to conjugated C=O and C=C stretching frequency groups; a band at 1546 cm^{-1} assigned to N–H bending and a band at 1227 cm^{-1} assigned to C–N of amine bonds. The FTIR spectrum of microspheres shows intense bands of C–H stretching close to 3000 cm^{-1} proceeding from MBA. Furthermore, the C=O band (1653 cm^{-1}) shifted to higher wavenumber due to a loss of conjugation of carboxyl groups after the crosslinking reaction. Two bands at 1549 and 1226 cm^{-1}, assigned respectively to N–H bending and to C–N of amine bonds proceeding from MBA, are observed in the microspheres FTIR spectrum.

Fig. 5a presents the TGA curves obtained for raw starch, starch-mod, MBA and microspheres. Two stages of weight loss are observed. The first one at ca. 50–150 °C attributed to the loss of water and other volatile compounds. In this stage the largest weight loss was verified for starch, indicating that the amount of moisture in its structure was greater than in starch-mod, microspheres or MBA. So as expected, starch is more hydrophilic than starch-mod, microspheres or MBA.

The second stage, in the range of 250–500 °C, was attributed to the thermal degradation of the samples. Fig. 5b shows the first derivate data (DTG) obtained from the TGA. The thermal stability decreases in the following order: MBA, raw starch, starch-mod and microspheres. Although, the starch-mod/MBA microspheres degrades at a lower temperature, at 600 °C the microspheres still had 20% of its initial weight while raw starch and starch-mod were completed degraded.

3.3. CUR loading and release assays

Despite CUR presents interesting activity against some types of human tumor, it presents a low bioavailability or poor absorption due to its slight solubility in water, which limits its oral administration (Sun et al., 2012). Other negative aspect is the CUR rapid metabolism and elimination, which decreases considerably the levels of CUR in serum and, as a consequence its bioavailability

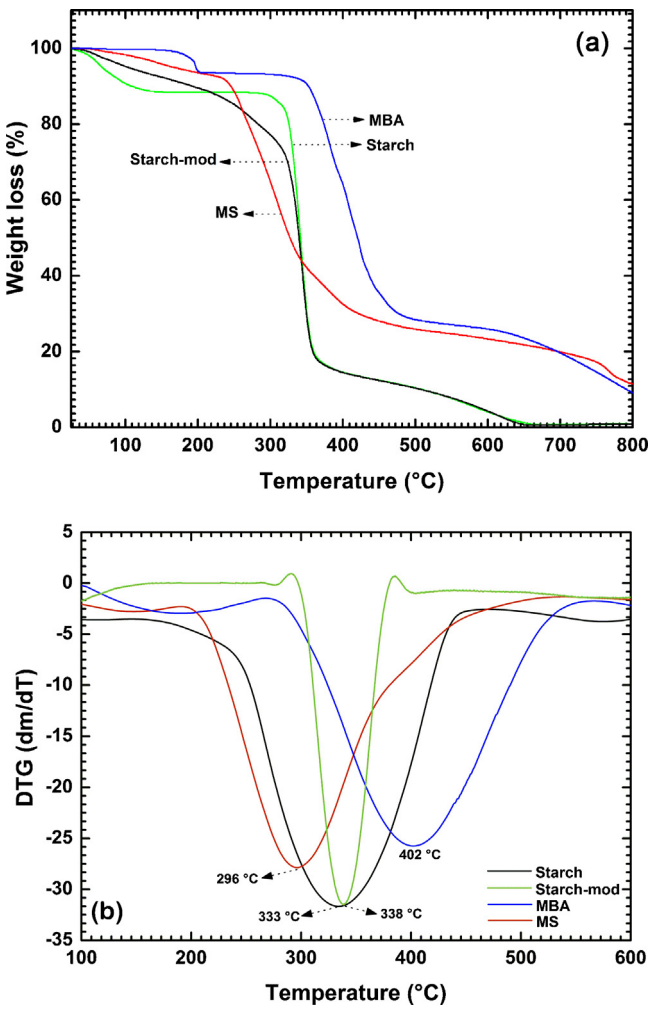

Fig. 5. (a) TGA and (b) DTG curves of starch-mod, microspheres (MS) and MBA.

(Johnson & Mukhtar, 2007; Tønnesen, Másson, & Loftsson, 2002). All this disadvantages limit its clinical application. One way to overcome these limitations and improve the oral bioavailability of CUR is to encapsulate it into a polymeric matrix, which acts as a device for controlling the drug release (Mohanty & Sahoo, 2010; Onofre & Wang, 2010). This is a well-known strategy that has been explored by several studies (Anand et al., 2007; Shaikh, Ankola, Beniwal, Singh, & Kumar, 2009). These studies show that when encapsulated into a polymeric matrix, the oral bioavailability of CUR is significantly enhanced (Shaikh et al., 2009).

Herein, CUR was encapsulated after microspheres preparation and it was not covalently bound to the matrix because the binding of drugs may be not achievable trivially and in such process there is a potential chance of original CUR pharmacological activity loss. Here, it is suggested that the interaction between the CUR and the microspheres matrix occurs by physical sorption, or Van der Waals sorption. This sorption phenomenon results from the weak attractive intermolecular forces between the solid molecules and the adsorbed substance. Its main characteristic is the reversible character, which allows the CUR to be released from the microspheres.

So, the microspheres were loaded through their immersion in a CUR solution. Through Eq. (1), CUR loading efficiency was estimated as ca. 90%, which means that 1.1 mg of CUR was encapsulated in 1.0 g of microspheres (0.1 wt/wt%).

The in vitro CUR release assays were carried out in two different media: simulated gastric and intestinal fluids (SGF and SIF). These

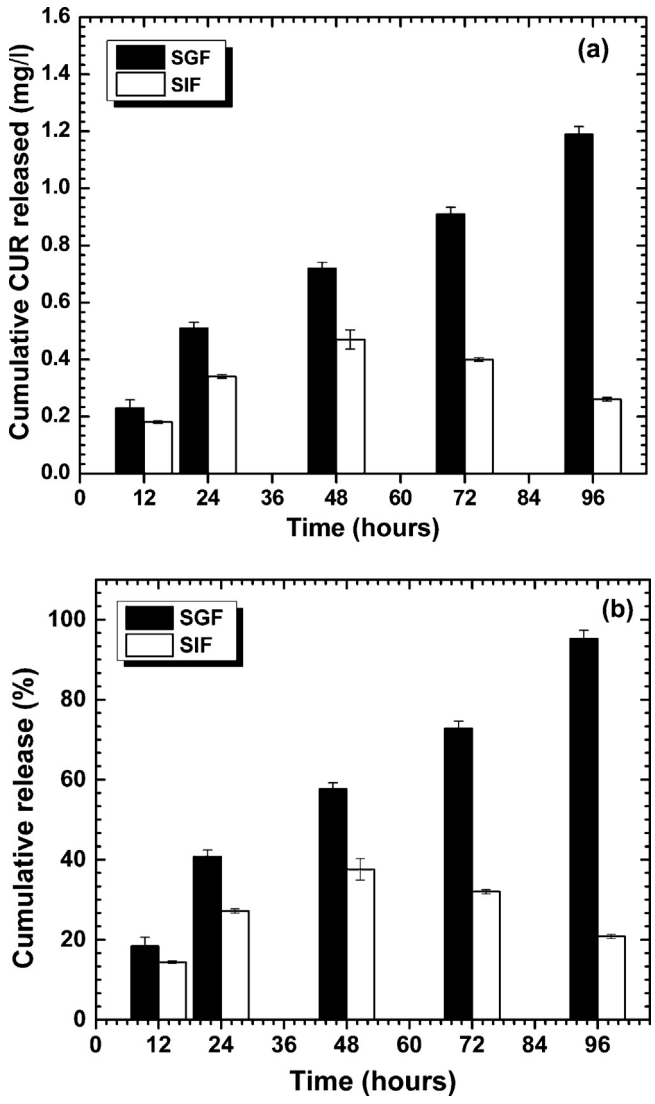

Fig. 6. Time-dependent cumulative CUR release in SGF (pH 1.2) and SIF (pH 6.8) [(a) in mg/l and (b) % in relation to the amount of CUR loaded].

media were chosen because they simulate some compartments, in which CUR-loaded microspheres have to pass when orally administrated. Aliquots were collected from the release media at specific time intervals and the maximum absorption of CUR (at 430 nm) was monitored by UV–vis spectra. The cumulative CUR release is shown in Fig. 6.

The data obtained from the in vitro CUR release assays showed the release profile is clearly pH-dependent and is more pronounced in acid condition. After 12 h in SGF, only 18% of encapsulated CUR was released from the microspheres, which increased up to 95% cumulative release by 96 h. On the other hand, in SIF a different release profile was observed. In the first 12 h, about 14% of CUR was released from the microspheres. The CUR cumulative release increased up to 38% by 48 h and then a drop in the concentration up to 20% was observed for 96 h. These data are in agreement with the work of Noack et al. that investigates the releasing of curcuminoids from loaded lipid nanoparticles (Noack, Oidtmann, Kutza, & Mäder, 2012).

According to Fig. 6 it could be inferred that the first CUR released might be relative to desorption process underwent by the adsorbed drug in the microsphere surfaces. As the microspheres have high surface area the CUR amount adsorbed is considerable high. The incessant contact between the SGF surface and releasing medium promoted faster dissolution and subsequently CUR was released through desorption process (Noack et al., 2012). For long immersion periods the CUR was released in a sustained manner due to the gradual release of the drug entrapped within the polymeric matrix. In addition, the higher release rate in SGF can be attributed to the increased solubility of the CUR under acid conditions when compared with neutral conditions (in SIF, for example) (Kakkar, Singh, Singla, & Kaur, 2011; Noack et al., 2012).

The CUR cumulative release data in SIF showed the release increased up to 38% by 48 h, which probably is referent to the release of the drug adsorbed at the microspheres surfaces. Once, CUR shows poor solubility in SIF, the drug encapsulated inside the microspheres network was not released. After 48 h of immersion in SIF, a decrease in the cumulative release was observed; this can be related to the degradation of the CUR in this medium. It is noteworthy that CUR is easily degraded when exposed to medium with pH close to or higher than 7. For this reason, it was inferred that the decreasing in the amount of CUR already released was most likely caused by degradation of CUR, which was released firstly from the microspheres surfaces, and/or the CUR degradation rate is higher than its releasing rate.

Besides, in order to evaluate the release profile of the drug, it is important to verify and understand the mechanism whereby the drug is released from the device applied in controlled release. The drug release from a polymeric device is nothing more than a mass transference of a solute from the device to the medium (solvent) and several factors affect this process (the geometry of the device, the immersion medium, the solute size, etc.). The mass transference is better understood when it is associated with diffusion laws. The Korsmeyer–Peppas model (Korsmeyer, Gurny, Doelker, Buri, & Peppas, 1983) allows to determinate the diffusion coefficient (n), a mathematical parameter that associates the release profile of a solute from an absorbable polymer network, as the starch-mod/MBA microspheres, for example. The model of Ritger–Peppas is described by Eq. (3) (Ritger & Peppas, 1987). It is important to report that equation 3 predicts the first 60% of released solute.

$$\frac{W_t}{W_{eq}} = kt^n \tag{3}$$

where W_t is the mass of solute released from the microspheres at a specified time interval and W_{eq} is the mass of solute released from the microspheres at equilibrium condition. k is a constant of proportionality that relates the characteristics of the polymeric network and the solute at a given solvent. n is a parameter that depends on the diffusion mechanism and it has different conceptual meaning depending on the geometrical shape of the release device (Guilherme et al., 2012; Thompson et al., 2006). For a spherical shape (which corresponds to the geometry of our microspheres) the value of the parameter n could be interpreted in the following way: (i) $n = 0.43$ for Fickian diffusion or Case I (the diffusion rate is slower than the relaxation of the polymeric chains); (ii) $0.43 < n < 0.86$ for anomalous transport, contribution of Fickian diffusion and controlled relaxation (the diffusion rate and the relaxation of the polymeric chains are similar), (iii) $n = 0.86$ for zero order or Case II (the diffusion rate is faster than the relaxation of the polymer chains) and (iv) $n > 0.86$ for super Case II (contribution of the macromolecular relaxation of the polymer chains in the diffusion process). The value of n was obtained from slope of the logarithmical curve of release (W_t/W_{eq}) ratio plotted against t, as shown in Fig. 7a. The value of n was obtained only to CUR-loaded starch-mod/MBA microspheres in SGF medium because in SIF the amount of CUR released did not achieve the equilibrium. The value obtained to n was equal to 0.73 ($R^2 = 0.943$), which demonstrates that the release mechanism of CUR from the microspheres is governed by anomalous transport or non-Fickian diffusion. This type of diffusion indicates a coupling of the diffusion and erosion controlled rate

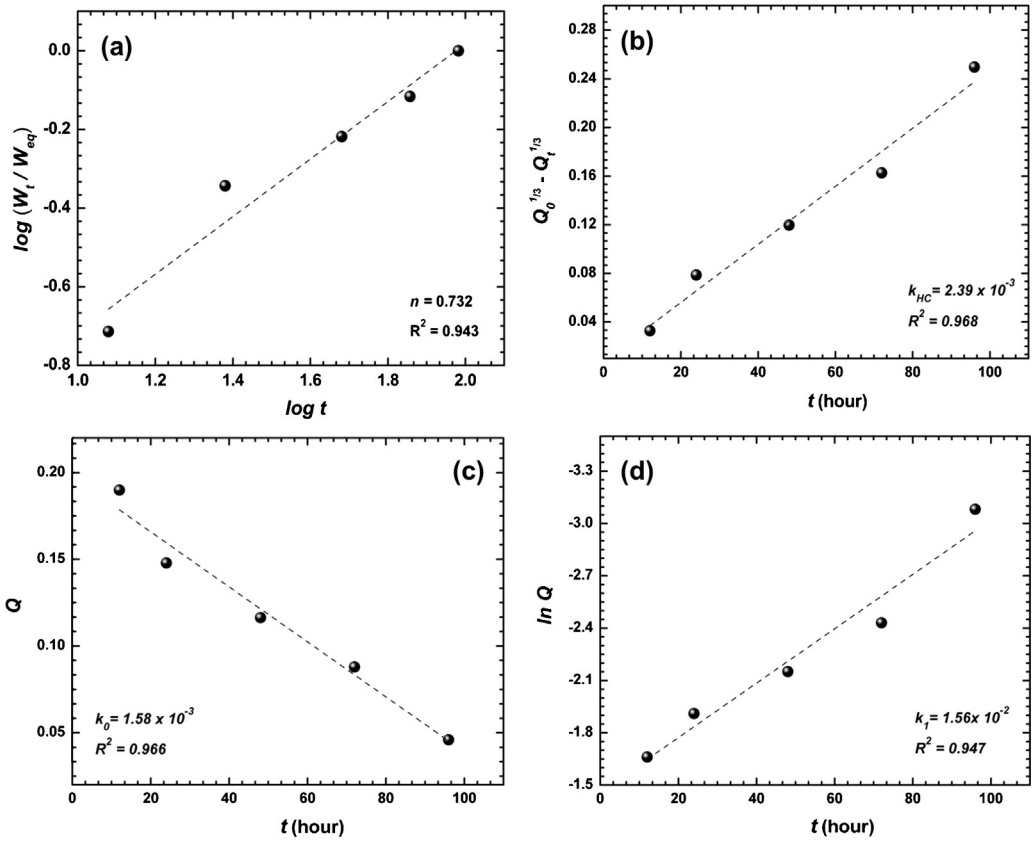

Fig. 7. (a) Korsmeyer–Peppas, (b) Hixson–Crowell, (c) zero-order, and (d) first-order release models.

release (Korsmeyer et al., 1983). To characterize the CUR release rate, the mean dissolution time (MDT) parameter was determined by Eq. (4), were k is the kinetic constant and n is the diffusional coefficient calculated from the Ritger and Peppas equation.

$$\mathrm{MDT} = \frac{n}{n+1}k^{-1/n} \tag{4}$$

The parameter MDT is a sum of the period of time that CUR molecules remain into the microspheres before release, divided by the total number of molecules of CUR encapsulated (Möckel & Lippold, 1993). The value of MDT calculated for $n = 0.73$ and $k = 3.57 \times 10^{-2}\ \mathrm{h}^{-1}$ was equal to 40 h and it indicates the efficiency of the polymer to retard the release of the drug.

Other important kinetic model is the Hixson–Crowell cube root law that describes the release from a system in which the surface area and diameter of the particles or tablets change caused by degradation or dissolution (Desai, Singh, Simonelli, & Higuchi, 1966; Singh, Desai, Simonelli, & Higuchi, 1967). For a drug powder consisting of uniformly sized particles, it is possible to derive an equation that expresses the rate of dissolution based on the cubic root of the particle, in this case, the microspheres. This equation is given as follows:

$$Q_0^{1/3} - Q_t^{1/3} = k_{\mathrm{HC}}t \tag{5}$$

where Q_0 is the amount of drug in the matrix at $t = 0$, Q_t is the amount of drug remaining in the matrix at time t, and k_{HC} is the cube root law rate constant. The value of k_{HC} was obtained from slope of the plot $Q_0^{1/3} - Q_t^{1/3}$ against t (in h), as shown in Fig. 7b. This model showed a correlation coefficient (R^2) of 0.968 indicating a change in the surface area and diameter of the microspheres as function of time. The drug diffuses out through an outer layer, which erodes allowing the water molecules to penetrate further into the core. The drug release is improved due to good solubilization of CUR in acid media (Colombo, Bettini, Santi, & Peppas, 2000; Costa, Valente, Miguel, & Queiroz, 2012).

Another important kinetic aspect is to understand whether the drug release is dependent or not on its concentration for a determined system. For this, CUR release kinetic was evaluated through zero-order and first-order release kinetics (Eqs. (6) and (7)). Zero-order release kinetics refers to the process of constant drug release from a drug delivery device such as oral osmotic tablets, transdermal systems, matrix tablets, matrix tablets with low-soluble drugs and other delivery systems (Gautam Singhvi, 2011). For the zero-order kinetics the release rate is non-dependent of drug concentration. Differently, the first-order release kinetics describes a release process where the drug concentration affects the release rate. In general terms, the zero- and first-order release kinetics can be described by the following equations:

$$Q = Q_0 - k_0 t \tag{6}$$

$$\ln\ Q = \ln Q_0 - k_1 t \tag{7}$$

where Q is the amount of drug released or dissolved (assuming that release occurs rapidly after the drug dissolves), Q_0 is the initial amount of drug encapsulated into the delivery system, and k_0 (h^{-1}) and k_1 (h^{-1}) are the zero- and first-order release constants. k_0 was obtained from slope of the plot Q against t (in h), and k_1 from the slope of the plot $\ln Q$ against t (in h), as shown in Fig. 7c and d. The R^2 value obtained for the zero-order is 0.968 and the constant k_0 is $1.58 \times 10^{-3}\ \mathrm{h}^{-1}$ and for the first-order R^2 and k_1 are 0.946 and $1.56 \times 10^{-2}\ \mathrm{h}^{-1}$, respectively. From these results it is possible to realize that the experimental data is better fitted by zero-order release kinetics model. Zero-order release kinetics for a delivery system is desirable because the release rate is constant minimizing any swing in drug concentration in the blood stream. In addition,

Table 1
In vitro evaluation of cytotoxic effects of CUR released from starch-mod/MBA microspheres on tumor cell lines.

Sample	In vitro cytotoxicity – CC_{50} (μg/ml)[a]	
	Caco-2 cells	HCT-116 cells
Control[b]	962 ± 23	300 ± 50
Pure CUR	38 ± 5	7.00 ± 0.14
C1[c]	0.85 ± 0.05	0.33 ± 0.06
C100[d]	62 ± 5	19 ± 5

[a] CC_{50} values were determined using sulforhodamine test and the data are means ± standard deviations from tests performed in triplicate ($n = 3$).
[b] Unloaded starch-mod/MBA microspheres were utilized as control.
[c] In this sample the amount of CUR encapsulated is 0.81 mg per gram of microspheres.
[d] In this sample the amount of CUR encapsulated is 82 mg per gram of microspheres.

this release profile leads to constant drug effect, provided the drug's pharmacokinetic and pharmacodynamic properties, such as distribution, metabolism, and elimination, and its pharmacodynamic properties relating plasma concentration to drug effect, are stationary.

3.4. Cytotoxic effect on tumor cell lines

Cancer could be characterized as a dysfunction of cell signaling due to a combination of genetic susceptibility and environmental exposure (Anand, Kunnumakkara, et al., 2008, Anand, Sundaram, Jhurani, Kunnumakkara, & Aggarwal, 2008b). CUR was proven to be an efficient drug in the fight of many tumor cell lines by acting at different stages in the development of affected cells (Anand, Sundaram, et al., 2008; Tang et al., 2010). The cytotoxicity effects of pure CUR, unloaded and CUR-loaded starch-mod/MBA microspheres were evaluated against both Caco-2 and HCT-116 cell lines and are displayed in Table 1. After 48 h of incubation, either free CUR or loaded microspheres exhibited inhibition effect on cell growth (CC_{50}) for both Caco-2 and HCT-116 cell lines, as compared to control group. Besides, the suppression on tumor cells growth showed to be dependent on levels of loading. In case of Caco-2 cells, the starch-mod/MBA microspheres containing the smallest amount of CUR (C1 ~ 1 mg/g) presented to be ca. 40 and 70 times more effective than pure CUR and C100 (~ 82 mg/g), respectively. In the case of HCT-116 cells, similar behavior was found. It has been shown that CUR is highly susceptible to degradation in aqueous solution even at physiological pH, and ca. 50% of CUR is degraded in cell culture medium supplemented with 10% of FBS in 8 h, while 90% is degraded in phosphate buffer pH 7.4 in 30 min (Shen & Ji, 2012; Wang et al., 1997). In light of this, the highest inhibitory effect on cellular growth presented by C1 in relation to pure CUR is attributed to the slower and constant release of CUR from the microspheres avoiding degradation and keeping the anti-tumor activity. It is not clear the reason why C100 was less effective than pure CUR or C1. Ma et al. (2008) and Song et al. (2011) report that CUR-loaded polymeric micelles presented similar cytotoxic effect toward different cell lines in relation to pure CUR at low concentration levels (2.5 and 5 μg/mL), but at higher concentrations the effect of pure CUR was greater than that observed for the CUR-loaded delivery system. This odd behavior was not explained.

It is believed that at higher concentrations (such C100) the physical state (amorphous or crystalline) of CUR inside the microspheres should be different from that at low concentration and thus, the releasing mechanism and the kinetic is probably different from C1, strongly influencing its cytotoxicity effect toward tumor cells. Therefore, further experiments are necessary to explain such behavior.

It is noteworthy to mention the microspheres prepared in this work increased the stability of CUR by protecting it against hydrolysis and the loss of CUR's pharmacologic activity. Besides, it is known that some inflammatory bowel diseases cause the decreasing in the pH of the colon. Therefore, the prepared microspheres, as showed by the pH dependence release, could be an interesting device for CUR-release in the treatment of colon cancer, when the disease decreases the local pH (Leopold & Eikeler, 2000).

Recently, different microparticles have been developed in order to protect and to deliver CUR in sustained fashion (Josephine Leno Jenita, Wilson, & Premakumari, 2012; Li, Li, & Li, 2011). It was showed by in vitro releasing profiles that such systems could modulate the delivery and degradation of CUR. However, cytotoxicity assays proving the efficacy of such systems against tumor cell lines were not presented. In this paper, the activity of CUR against Caco-2 and HCT-116 tumor cells was demonstrated and could be outstanding improved when CUR is encapsulated in starch-mod/MBA microspheres, and this effect is dependent on loading level. Therefore, this study shows an interesting contribution to the field presenting a new release system based on the biopolymer starch.

4. Conclusions

Original starch based microspheres were successfully prepared by emulsion method to be applied as device for controlled release of curcumin (CUR). Raw starch was modified by grafting vinyl groups from glycidyl methacrylate (GMA), as confirmed by FTIR (1718 cm^{-1} assigned to C = O) and ^1H NMR at δ 6.17 and δ 5.64 ppm which were attributed to hydrogen bounded to vinyl group. SEM images demonstrated uniform size distribution ca. 400–500 μm. The microspheres showed to be a very promising device for the controlled release of CUR, especially for the treatment of colon cancer, which in general decreases the pH of the colon. At simulated intestinal fluid the polymer matrix did not expand avoiding the influx of fluid and consequently the release of CUR. In that condition only the CUR adsorbed on the microspheres surface was released at the first day decreasing its concentration in the following days. However, at simulated gastric fluid the fraction released of CUR was 100% and in a controlled manner, due to the sustained diffusion of CUR to the media and also due to the degradation of the polymer matrix. The CUR-loaded microspheres presented much higher activity against Caco-2 and HCT-116 tumor cell lines than free CUR.

References

Anand, P., Kunnumakkara, A. B., Newman, R. A., & Aggarwal, B. B. (2007). Bioavailability of curcumin: Problems and promises. *Molecular Pharmaceutics*, *4*(6), 807–818.

Anand, P., Kunnumakkara, A. B., Sundaram, C., Harikumar, K. B., Tharakan, S. T., Lai, O. S., et al. (2008). Cancer is a preventable disease that requires major lifestyle changes. *Pharmaceutical Research*, *25*(9), 2097–2116.

Anand, P., Sundaram, C., Jhurani, S., Kunnumakkara, A. B., & Aggarwal, B. B. (2008). Curcumin and cancer: an "old-age" disease with an "age-old" solution. *Cancer Letters*, *267*(1), 133–164.

Angellier, H., Molina-Boisseau, S., Dole, P., & Dufresne, A. (2006). Thermoplastic starch—waxy maize starch nanocrystals nanocomposites. *Biomacromolecules*, *7*(2), 531–539.

Cabrespine-Faugeras, A., Bayet-Robert, M., Bay, J. O., Chollet, P., & Barthomeuf, C. (2010). Possible benefits of curcumin regimen in combination with taxane chemotherapy for hormone-refractory prostate cancer treatment. *Nutrition and Cancer*, *62*(2), 148–153.

Chen, L., Li, X., Pang, Y., Li, L., Zhang, X., & Yu, L. (2007). Resistant starch as a carrier for oral colon-targeting drug matrix system. *Journal of Materials Science: Materials in Medicine*, *18*(11), 2199–2203.

Colombo, P., Bettini, R., Santi, P., & Peppas, N. A. (2000). Swellable matrices for controlled drug delivery: gel-layer behaviour, mechanisms and optimal performance. *Pharmaceutical Science & Technology Today*, *3*(6), 198–204.

Costa, D., Valente, A. J. M., Miguel, M. G., & Queiroz, J. (2012). Plasmid DNA microgels for a therapeutical strategy combining the delivery of genes and anticancer drugs. *Macromolecular Bioscience*, *12*(9), 1243–1252.

Costa, E., De-Carvalho, J., Casimiro, T., Da Silva, C. L., Cidade, M. T., & Aguiar-Ricardo, A. (2011). Tailoring thermoresponsive microbeads in supercritical carbon dioxide for biomedical applications. *Journal of Supercritical Fluids*, *56*(3), 292–298.

Desai, S. J., Singh, P., Simonelli, A. P., & Higuchi, W. I. (1966). Investigation of factors influencing release of solid drug dispersed in inert matrices III. Quantitative studies involving the polyethylene plastic matrix. *Journal of Pharmaceutical Sciences*, *55*(11), 1230–1234.

Gautam Singhvi, M. S. (2011). Review: In-vitro drug release characterization models. *International Journal of Pharmaceutical Studies and Research*, *2*(1), 77–84.

Guilherme, M. R., Oliveira, R. S., Mauricio, M. R., Cellet, T. S. P., Pereira, G. M., Kunita, M. H., et al. (2012). Albumin release from a brain-resembling superabsorbent magnetic hydrogel based on starch. *Soft Matter*, *8*(24), 6629–6637.

Guilherme, M. R., Reis, A. V., Takahashi, S. H., Rubira, A. F., Feitosa, J. P. A., & Muniz, E. C. (2005). Synthesis of a novel superabsorbent hydrogel by copolymerization of acrylamide and cashew gum modified with glycidyl methacrylate. *Carbohydrate Polymers*, *61*(4), 464–471.

Hedin, J., Östlund, A., & Nydén, M. (2010). UV induced cross-linking of starch modified with glycidyl methacrylate. *Carbohydrate Polymers*, *79*(3), 606–613.

Huang, J., Schols, H. A., Klaver, R., Jin, Z., & Voragen, A. G. J. (2007). Acetyl substitution patterns of amylose and amylopectin populations in cowpea starch modified with acetic anhydride and vinyl acetate. *Carbohydrate Polymers*, *67*(4), 542–550.

Jain, A., Gupta, Y., & Jain, S. K. (2007). Perspectives of biodegradable natural polysaccharides for site-specific drug delivery to the colon. *Journal of Pharmacy and Pharmaceutical Sciences*, *10*(1), 86–128.

Johnson, J. J., & Mukhtar, H. (2007). Curcumin for chemoprevention of colon cancer. *Cancer Letters*, *255*(2), 170–181.

Josephine Leno Jenita, J., Wilson, Y. M., & Premakumari KB, B. (2012). Formulation and evaluation of microparticles containing curcumin for colorectal cancer. *Journal of Drug Delivery & Therapeutics*, *2*(3), 125–128.

Kakkar, V., Singh, S., Singla, D., & Kaur, I. P. (2011). Exploring solid lipid nanoparticles to enhance the oral bioavailability of curcumin. *Molecular Nutrition & Food Research*, *55*(3), 495–503.

Kim, C. H., Cho, K. Y., & Park, J. K. (2001). Reactive blends of gelatinized starch and polycaprolactone-g-glycidyl methacrylate. *Journal of Applied Polymer Science*, *81*(6), 1507–1516.

Kizil, R., Irudayaraj, J., & Seetharaman, K. (2002). Characterization of irradiated starches by using FT-Raman and FTIR spectroscopy. *Journal of Agricultural and Food Chemistry*, *50*(14), 3912–3918.

Korsmeyer, R. W., Gurny, R., Doelker, E., Buri, P., & Peppas, N. A. (1983). Mechanisms of solute release from porous hydrophilic polymers. *International Journal of Pharmaceutics*, *15*(1), 25–35.

Leopold, C. S., & Eikeler, D. (2000). Basic coating polymers for the colon-specific drug delivery in inflammatory bowel disease. *Drug Development and Industrial Pharmacy*, *26*(12), 1239–1246.

Li, F., Li, X., & Li, B. (2011). Preparation of magnetic polylactic acid microspheres and investigation of its releasing property for loading curcumin. *Journal of Magnetism and Magnetic Materials*, *323*(22), 2770–2775.

Ma, Z., Haddadi, A., Molavi, O., Lavasanifar, A., Lai, R., & Samuel, J. (2008). Micelles of poly(ethylene oxide)-b-poly(ε-caprolactone) as vehicles for the solubilization, stabilization, and controlled delivery of curcumin. *Journal of Biomedical Materials Research Part A*, *86A*(2), 300–310.

Mandal, B. B., Kapoor, S., & Kundu, S. C. (2009). Silk fibroin/polyacrylamide semi-interpenetrating network hydrogels for controlled drug release. *Biomaterials*, *30*(14), 2826–2836.

Mandeville, J.-S., Froehlich, E., & Tajmir-Riahi, H. A. (2009). Study of curcumin and genistein interactions with human serum albumin. *Journal of Pharmaceutical and Biomedical Analysis*, *49*(2), 468–474.

Meng, L. M., Yuan, Y. C., Rong, M. Z., & Zhang, M. Q. (2010). A dual mechanism single-component self-healing strategy for polymers. *Journal of Materials Chemistry*, *20*(29), 6030–6038.

Möckel, J., & Lippold, B. (1993). Zero-order drug release from hydrocolloid matrices. *Pharmaceutical Research*, *10*(7), 1066–1070.

Mohanty, C., & Sahoo, S. K. (2010). The in vitro stability and in vivo pharmacokinetics of curcumin prepared as an aqueous nanoparticulate formulation. *Biomaterials*, *31*(25), 6597–6611.

Namazi, H., & Dadkhah, A. (2010). Convenient method for preparation of hydrophobically modified starch nanocrystals with using fatty acids. *Carbohydrate Polymers*, *79*(3), 731–737.

Noack, A., Oidtmann, J., Kutza, J., & Mäder, K. (2012). In vitro digestion of curcuminoid-loaded lipid nanoparticles. *Journal of Nanoparticle Research*, *14*(9).

Onofre, F. O., & Wang, Y. J. (2010). Sustained release properties of crosslinked and substituted starches. *Journal of Applied Polymer Science*, *117*(3), 1558–1565.

Skehan, P., Scudeiro, R. S. D., Monks, A., McMahon, J., Vistica, D., Warren, J. T., et al. (1990). New colorimetric cytotoxicity assay for anticancer-drug screening. *Journal of National Cancer Institute*, *82*(13), 1107–1112.

Pereira, A. G. B., Gouveia, R. F., de Carvalho, G. M., Rubira, A. F., & Muniz, E. C. (2009). Polymer blends based on PEO and starch: Miscibility and spherulite growth rate evaluated through DSC and optical microscopy. *Materials Science and Engineering C*, *29*(2), 499–504.

Radhakrishna Pillai, G., Srivastava, A. S., Hassanein, T. I., Chauhan, D. P., & Carrier, E. (2004). Induction of apoptosis in human lung cancer cells by curcumin. *Cancer Letters*, *208*(2), 163–170.

Reis, A. V., Fajardo, A. R., Schuquel, I. T. A., Guilherme, M. R., Vidotti, G. J., Rubira, A. F., et al. (2009). Reaction of glycidyl methacrylate at the hydroxyl and carboxylic groups of poly(vinyl alcohol) and poly(acrylic acid): Is this reaction mechanism still unclear? *The Journal of Organic Chemistry*, *74*(10), 3750–3757.

Reis, A. V., Guilherme, M. R., Moia, T. A., Mattoso, L. H. C., Muniz, E. C., & Tambourgi, E. B. (2008). Synthesis and characterization of a starch-modified hydrogel as potential carrier for drug delivery system. *Journal of Polymer Science. Part A: Polymer Chemistry*, *46*(7), 2567–2574.

Ritger, P. L., & Peppas, N. A. (1987). A simple equation for description of solute release I. Fickian and non-Fickian release from non-swellable devices in the form of slabs, spheres, cylinders or discs. *Journal of Controlled Release*, *5*(1), 23–36.

Riyajan, S. A., Sasithornsonti, Y., & Phinyocheep, P. (2012). Green natural rubber-g-modified starch for controlling urea release. *Carbohydrate Polymers*, *89*(1), 251–258.

Rodrigues, F. A., Fajardo, A., Pereira, A. B., Ricardo, N. P. S., Feitosa, J. A., & Muniz, E. (2012). Chitosan-graft-poly(acrylic acid)/rice husk ash based superabsorbent hydrogel composite: preparation and characterization. *Journal of Polymer Research*, *19*(12), 1–10.

Sahu, A., Bora, U., Kasoju, N., & Goswami, P. (2008). Synthesis of novel biodegradable and self-assembling methoxy poly(ethylene glycol)-palmitate nanocarrier for curcumin delivery to cancer cells. *Acta Biomaterialia*, *4*(6), 1752–1761.

Saito, N., Murakami, N., Takahashi, J., Horiuchi, H., Ota, H., Kato, H., et al. (2005). Synthetic biodegradable polymers as drug delivery systems for bone morphogenetic proteins. *Advanced Drug Delivery Reviews*, *57*(7), 1037–1048.

Shaikh, J., Ankola, D. D., Beniwal, V., Singh, D., & Kumar, M. N. V. R. (2009). Nanoparticle encapsulation improves oral bioavailability of curcumin by at least 9-fold when compared to curcumin administered with piperine as absorption enhancer. *European Journal of Pharmaceutical Sciences*, *37*(3–4), 223–230.

Sharma, R. A., Gescher, A. J., & Steward, W. P. (2005). Curcumin: the story so far. *European Journal of Cancer*, *41*(13), 1955–1968.

Shen, L., & Ji, H. F. (2012). The pharmacology of curcumin: Is it the degradation products? *Trends in Molecular Medicine*, *18*(3), 138–144.

Singh, P., Desai, S. J., Simonelli, A. P., & Higuchi, W. I. (1967). Release rates of solid drug mixtures dispersed in inert matrices. I. Noninteracting drug mixtures. *Journal of Pharmaceutical Sciences*, *56*(12), 1542–1547.

Song, L., Shen, Y., Hou, J., Lei, L., Guo, S., & Qian, C. (2011). Polymeric micelles for parenteral delivery of curcumin: preparation, characterization and in vitro evaluation. *Colloids and Surfaces A: Physicochemical and Engineering Aspects*, *390*(1–3), 25–32.

Spagnol, C., Rodrigues, F. A., Pereira, A. B., Fajardo, A., Rubira, A., & Muniz, E. (2012). Superabsorbent hydrogel nanocomposites based on starch-g-poly(sodium acrylate) matrix filled with cellulose nanowhiskers. *Cellulose*, *19*(4), 1225–1237.

Spagnol, C., Rodrigues, F. H. A., Neto, A. G. V. C., Pereira, A. G. B., Fajardo, A. R., Radovanovic, E., et al. (2012). Nanocomposites based on poly(acrylamide-co-acrylate) and cellulose nanowhiskers. *European Polymer Journal*, *48*(3), 454–463.

Sun, A., Shoji, M., Lu, Y. J., Liotta, D. C., & Snyder, J. P. (2006). Synthesis of EF24-tripeptide chloromethyl ketone: A novel curcumin-related anticancer drug delivery system. *Journal of Medicinal Chemistry*, *49*(11), 3153–3158.

Sun, M., Zhao, L., Guo, C., Cao, F., Chen, H., Zhao, L., et al. (2012). Evaluation of an oral carrier system in rats: Bioavailability and gastrointestinal absorption properties of curcumin encapsulated PBCA nanoparticles. *Journal of Nanoparticle Research*, *14*.(2).

Tang, H., Murphy, C. J., Zhang, B., Shen, Y., Van Kirk, E. A., Murdoch, W. J., et al. (2010). Curcumin polymers as anticancer conjugates. *Biomaterials*, *31*(27), 7139–7149.

Thompson, M. T., Berg, M. C., Tobias, I. S., Lichter, J. A., Rubner, M. F., & Van Vliet, K. J. (2006). Biochemical functionalization of polymeric cell substrata can alter mechanical compliance. *Biomacromolecules*, *7*(6), 1990–1995.

Tønnesen, H. H., Másson, M., & Loftsson, T. (2002). Studies of curcumin and curcuminoids. XXVII. Cyclodextrin complexation: Solubility, chemical and photochemical stability. *International Journal of Pharmaceutics*, *244*(1–2), 127–135.

Vemula, P. K., Cruikshank, G. A., Karp, J. M., & John, G. (2009). Self-assembled prodrugs: An enzymatically triggered drug-delivery platform. *Biomaterials*, *30*(3), 383–393.

Wang, Y. J., Pan, M. H., Cheng, A. L., Lin, L. I., Ho, Y. S., Hsieh, C. Y., et al. (1997). Stability of curcumin in buffer solutions and characterization of its degradation products. *Journal of Pharmaceutical and Biomedical Analysis*, *15*(12), 1867–1876.

Xu, Y., Ding, W., Liu, J., Li, Y., Kennedy, J. F., Gu, Q., et al. (2010). Preparation and characterization of organic-soluble acetylated starch nanocrystals. *Carbohydrate Polymers*, *80*(4), 1078–1084.

Zhang, B., Gong, H., Lü, S., Ni, B., Liu, M., Gao, C., et al. (2012). Synthesis and characterization of carboxymethyl potato starch and its application in reactive dye printing. *International Journal of Biological Macromolecules*, *51*(4), 668–674.